



This is a repository copy of *Strain Balancing of Metal-Organic Vapour Phase Epitaxy InAs/GaAs Quantum Dot Lasers*.

White Rose Research Online URL for this paper:
<http://eprints.whiterose.ac.uk/119609/>

Version: Accepted Version

Article:

Roberts, T.S., Stevens, B.J., Clarke, E. et al. (8 more authors) (2017) Strain Balancing of Metal-Organic Vapour Phase Epitaxy InAs/GaAs Quantum Dot Lasers. *IEEE Journal of Selected Topics in Quantum Electronics*, 23 (6). 1901208. ISSN 1077-260X

<https://doi.org/10.1109/JSTQE.2017.2703666>

© 2017 IEEE. Personal use of this material is permitted. Permission from IEEE must be obtained for all other users, including reprinting/ republishing this material for advertising or promotional purposes, creating new collective works for resale or redistribution to servers or lists, or reuse of any copyrighted components of this work in other works

Reuse

Items deposited in White Rose Research Online are protected by copyright, with all rights reserved unless indicated otherwise. They may be downloaded and/or printed for private study, or other acts as permitted by national copyright laws. The publisher or other rights holders may allow further reproduction and re-use of the full text version. This is indicated by the licence information on the White Rose Research Online record for the item.

Takedown

If you consider content in White Rose Research Online to be in breach of UK law, please notify us by emailing eprints@whiterose.ac.uk including the URL of the record and the reason for the withdrawal request.



eprints@whiterose.ac.uk
<https://eprints.whiterose.ac.uk/>

Strain Balancing Of Metal-Organic Vapour Phase Epitaxy InAs/GaAs Quantum Dot Lasers

Timothy S. Roberts, Benjamin J. Stevens, Edmund Clarke, Ian Tooley, Jonathan Orchard, Ian Farrer, David T.D Childs, Nasser Babazadeh, Nobuhiko Ozaki, David Mowbray, Richard A. Hogg

Abstract—Incorporation of a $\text{GaAs}_{0.8}\text{P}_{0.2}$ layer allows strain balancing to be achieved in self-assembled InAs/GaAs quantum dots (QDs) grown by metal organic vapour phase epitaxy (MOVPE). Tuneable wavelength and high density are obtained through growth parameter optimisation, with emission at $1.27\mu\text{m}$ and QD layer density $3 \times 10^{10}\text{cm}^{-2}$. Strain balancing allows close vertical stacking (30nm) of the QD layers, giving the potential for increased optical gain. Modelling and device characterisation indicates minimal degradation in the optical and electrical characteristics unless the phosphorus percentage is increased above 20%. Laser structures are fabricated with a layer separation of 30nm, demonstrating low temperature lasing with a threshold current density of 100A/cm^2 at 130K without any facet coating.

Index Terms—MOCVD, MOVPE, Quantum Dots, Strain Balancing, Stranski-Krastanov, Semiconductor Laser

I. INTRODUCTION

Quantum dots (QDs) have been of considerable interest over the past 35 years since the prediction of Arakawa and Sakaki of their potential benefits for lasers [1]. A number of research groups have reported the growth of self-assembled QDs by metal organic vapour phase epitaxy (MOVPE), including reports of ground state lasing at room temperature [2]-[10]. Increasing the ground state wavelength towards $1.3\mu\text{m}$ has been a challenge but has been achieved with the introduction of a strain reducing layer (SRL) [11]-[17]. Whilst the InGaAs SRL has the desired effect of an increase in wavelength by reducing the localised strain of the QDs, additional indium increases the overall strain into the active region [18]. This strain limits the minimum separation between layers and hence the maximum number of active layers achievable. Exceeding this limit results in the formation of dislocations, which significantly degrade the optical and electrical properties. Strain compensation using tensile materials, such as GaP have been studied in both molecular beam epitaxy (MBE) [19] and MOVPE [20]-[23], with room temperature ground state lasing reported

This work was supported by the EPSRC under Grant EP/I018328/1.

T. S. Roberts, E. Clarke, I. Tooley, I. Farrer and D. Mowbray, are with the University Of Sheffield, S3, UK. (e-mail: tim.roberts@sheffield.ac.uk, edmund.clarke@sheffield.ac.uk, ian.tooley@sheffield.ac.uk, i.farrer@sheffield.ac.uk, d.mowbray@sheffield.ac.uk)

B. J. Stevens, was with the University of Sheffield, Sheffield, S3 7HQ, UK. He is now with IQE (e-mail:bstevens@iqep.com)

J. Orchard, D. T. D Childs, N. Babazadeh and R. A. Hogg were with the University of Sheffield, Sheffield, S3 7HQ, UK but now are with Glasgow University, Glasgow, G12 8QQ, UK. (e-mail: jonathan.orchard@glasgow.ac.uk, david.childs@glasgow.ac.uk, nasser.babazadeh@glasgow.ac.uk, richard.hogg@glasgow.ac.uk)

N. Ozaki was with the University of Sheffield, Sheffield, S3 7HQ, UK, on leave from Wakayama University, Wakayama, Japan (e-mail: ozaki@sys.wakayama-u.ac.jp).

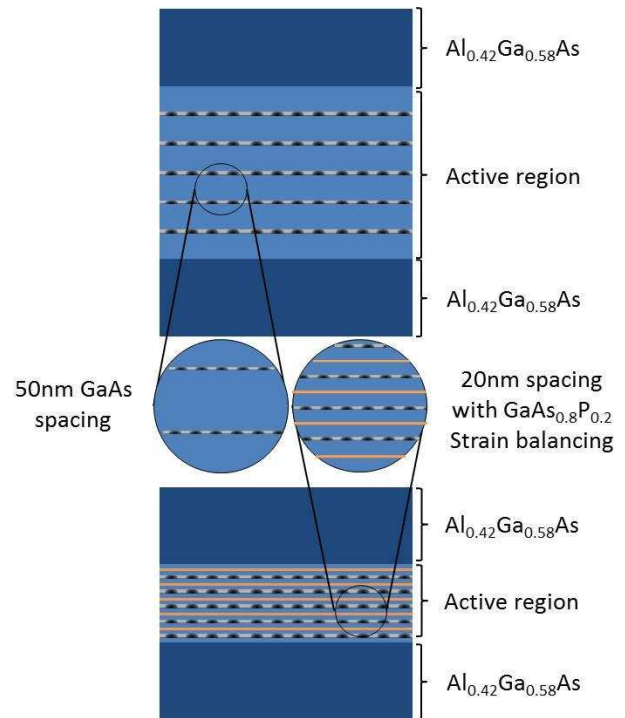


Fig. 1. Schematic of the strain balancing scheme discussed in this paper.

[5]. However, introduction of these strain compensation layers is detrimental to the electrical characteristics as revealed by device modelling (section III). An alternative approach, previously reported, is the incorporation of QDs directly into a $\text{GaAs}_{1-x}\text{P}_x$ matrix. However, this causes an unwanted blue shift in emission wavelength [24], [25]. In the present work the design of a strain balancing layer, which compensates all of the QD strain but does not adversely affect the device characteristics, is presented.

With the introduction of a suitable strain balancing layer the total internal strain can be reduced close to zero, allowing close vertical stacking and increasing the number of QD layers that can be placed close to the maximum of the cavity mode, hence achieving a higher total gain. Figure 1 shows an active region schematic with zero net strain via the incorporation of a $\text{GaAs}_{0.8}\text{P}_{0.2}$ strain balancing layer. Achieving a net strain of zero for each repeat of a QD layer plus strain balancing layer allows the separation between the QD layers to be reduced. For a layer QD areal density of $3 \times 10^{10}\text{cm}^{-2}$, reducing the separation from 50 to 20 nm will increase the volumetric density by 2.5 times from 6×10^{15} to $1.5 \times 10^{16}\text{cm}^{-3}$. Devices containing phosphide materials are less commonly grown by MBE due to the difficulty in phosphorous management; this is not an issue for MOVPE. Furthermore, MOVPE lends itself to large scale

manufacturing, due to the high uptime and volume scalability. In addition, epitaxial regrowth is significantly more mature in MOVPE with polycrystalline free selective area regrowth being highly challenging for MBE. The strain balancing described in this paper may also find application in solar cells, due to the large number of QD layers needed. This paper reports the successful incorporation of a GaAs_{0.8}P_{0.2} strain balancing layer into MOVPE grown laser structures. A five layer, 30 nm spacing strain balanced QD laser grown by MOVPE operating up to 200K without any facet coating is demonstrated. Section II of this paper describes the QD growth optimisation process including how growth rate and arsine flow affect the QD characteristics. Section III outlines the strain balancing process, modelling the IV characteristics to show degradation in turn-on voltage with increasing phosphorus percentage above 20%. Section IV discusses the low temperature lasing characteristics of three different devices. Lasing at elevated temperatures is inhibited due to a wide spread in QD emission energies arising from a bimodal distribution of dot size. Section V proposes a modification of the growth parameters to overcome this issue.

II. QUANTUM DOT GROWTH AND OPTIMISATION

InAs is deposited onto GaAs with a 7% mismatch in their lattice parameters. This mismatch creates a highly strained 2D layer of InAs below the critical thickness but as more InAs is added pseudomorphic growth is replaced by 3D growth; the Stranski-Krastanov (S-K) growth mode. Each growth parameter is characterised to understand how the QDs are affected. All devices are grown on 2" Si doped GaAs substrates (001), cut 3° off toward (110). TMIIn, TMAI, TMGa and arsine are used as precursors. For initial structures for photo-luminescence (PL) characterisation, following the growth of a GaAs buffer layer, a lower cladding layer of 150nm Al_{0.42}Ga_{0.58}As was grown, followed by a 60nm GaAs active region, with the QD layer placed in the centre. The InAs QDs were capped with 8nm low temperature grown GaAs followed by a temperature ramp to 530°C and the completion of the capping layer. An upper cladding layer of 150nm Al_{0.42}Ga_{0.58}As and a 30nm GaAs cap completed the structure. The QD layer was grown at 485°C, by deposition of 2.0ML of InAs at a growth rate of 0.04ML/s and initial V/III ratios of 910 and 95 during QD growth and capping layer growth, respectively. A series of samples were grown either varying the growth rate or the arsine flows during QD growth or capping. For structures to study the effect of stacking QD layers, the number of layers was increased to five, with a separation of 50nm of GaAs between layers. Laser devices were p-i-n structures containing five QD layers within the intrinsic active region and 1.5μm Al_{0.42}Ga_{0.58}As n and p doped (1x10¹⁸ and 5x10¹⁷) cladding regions. PL measurements were obtained at room temperature using a 532nm laser and under low excitation power (0.38mW) to avoid excited state emission. The light is coupled into a monochromator and detected using an InGaAs detector.

The effect of growth rate on peak PL wavelength is shown in Figure 2(a). As the growth rate decreases from 0.18ML/s to 0.04ML/s a red-shift is observed in the ground state wavelength from 1.22 to 1.24μm, producing 20nm

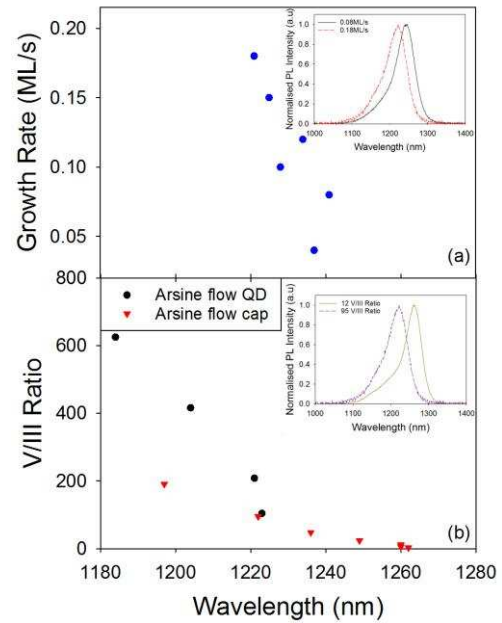


Fig. 2(a). Room temperature peak PL wavelength for different growth rates (inset) Room temperature low power PL of two samples for different growth rates.

Fig. 2(b). Room temperature peak PL wavelength for different III/V ratios. (inset) Room temperature PL with low excitation power obtained from two samples with different III/V ratio during the capping layer growth.

tunability. The inset to Figure 2 (a) shows normalised PL spectra for 0.08ML/s and 0.18ML/s. Cross-sectional transmission electron microscopy (TEM) estimated QD density measurements were performed using 113 dark field imaging conditions as described in [26]; because of the random positions of the QDs this may under-estimate the true density but should allow a relative comparison between different samples. A decrease in dot density with decreasing growth rate is observed; from $2.5 \times 10^{10} \text{cm}^{-2}$ at 0.18ML/s to $4.5 \times 10^9 \text{cm}^{-2}$ at 0.08ML/s. The extension in wavelength and lower QD density with reduced growth rate is due to the deposited InAs forming larger, more indium rich dots [27].

To achieve ground state lasing a high QD density is

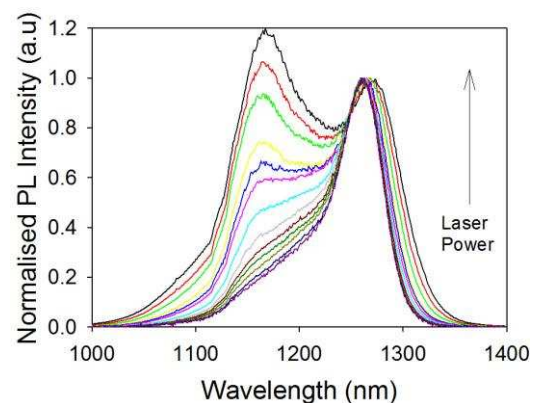


Fig. 3. Normalised room temperature power dependent PL of the 5 layer sample with nominal optimum growth conditions.

required, therefore for subsequent optimisation the highest growth rate of 0.18ML/s was used. The effect of arsine flow during both QD and capping growth is shown in Figure 2 (b). First, the effect of arsine flow during QD growth will be discussed. As the V/III ratio is increased from 104 to 625 a reduction is observed in the ground state emission from 1.22 to 1.18μm, however an unexpected decrease in QD density

is also observed; from $2.5 \times 10^{10} \text{cm}^{-2}$ for a V/III ratio of 208 to $1 \times 10^{10} \text{cm}^{-2}$ for a V/III ratio of 625. Due to this observed drop in QD density, subsequent samples used a V/III ratio of 104 for the QD growth.

The effect of the V/III ratio during the capping layer growth was studied due to surface morphology issues, found after stacking five QD layers. Unexpectedly, the V/III ratio during the capping layer significantly affected the ground state wavelength. Therefore, the V/III ratio during capping growth was explored. The V/III ratio was changed from 2.8 to 190 for both the initial 8nm cap and the subsequent 42nm GaAs spacing layer. As the V/III ratio is decreased from 190 to 2.8, an increase in ground state emission wavelength is observed, from 1.197 to $1.262 \mu\text{m}$, as shown in Figure 2 (b). TEM images indicate a constant QD density of $2.5 \times 10^{10} \text{cm}^{-2}$ for samples grown using V/III ratios between 95 and 12. The mechanism behind the extension in wavelength is currently unknown but is a useful process to increasing the wavelength without using an SRL. The inset to Figure 2 (b) shows the increase in wavelength from 1.22 to $1.26 \mu\text{m}$ using a V/III ratio of 95 and 12 respectively.

After optimising the growth conditions focus shifted towards developing QD laser devices. Figure 3 shows room temperature power dependent PL spectra of a five-layer sample with a QD layer separation of 50nm. Two peaks are observed, associated with the ground state and excited state emission at 1.27 and $1.165 \mu\text{m}$ respectively, producing a relatively large state separation of 88meV and a linewidth of 55meV. A high energy shoulder at low power is observed on the ground state. A red shifting of the emission, associated with thermal effects, is observed at high pump power.

Figure 4 shows a typical cross-sectional TEM image of the QDs. All samples show QDs with a similar size and

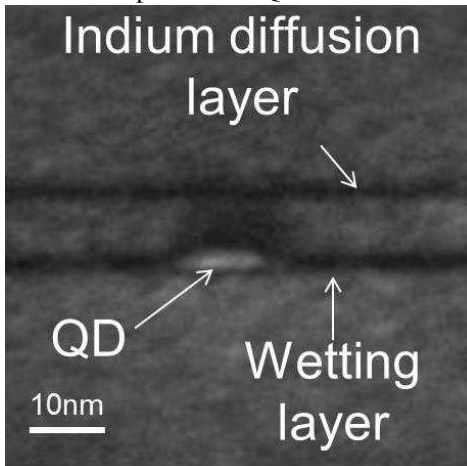


Fig. 4. TEM image of a QD grown at 485°C with 2ML InAs coverage, 0.18ML/s Growth Rate, 50sccm arsine flow.

shape, nucleated on a wetting layer. The samples also show an indium diffusion layer which accumulates at the top of the low temperature grown GaAs cap. The mechanism behind the formation of this layer is unclear and how this layer affects carrier capture and recombination mechanisms remains to be studied. Attempts at removing this layer by increasing the thickness of the low temperature cap to 15nm and applying a temperature increase to 580°C to flush indium from the surface has not been successful.

TABLE I

Sample	Separation	Strain Balancing	Θ_{sub}	Z_0
A	50nm	No	33.03°	32.9769°
A'	50nm	Yes	33.0302°	33.02°
B	30nm	No	33.0314°	32.9294°
B'	30nm	Yes	33.03°	33.0234°

III. STRAIN BALANCING

Table 1 gives the parameters of four samples grown using the optimised growth conditions but with the introduction of a $\text{GaAs}_{0.8}\text{P}_{0.2}$ strain balancing layer. Sample A is a five layer 50nm separation device without $\text{GaAs}_{0.8}\text{P}_{0.2}$, sample A' has the same parameters except that a 5nm $\text{GaAs}_{0.8}\text{P}_{0.2}$ layer is placed in the centre of the GaAs spacer layer after each QD layer. Samples B and B' follow A and A' except that the QD layer separation is reduced to 30nm.

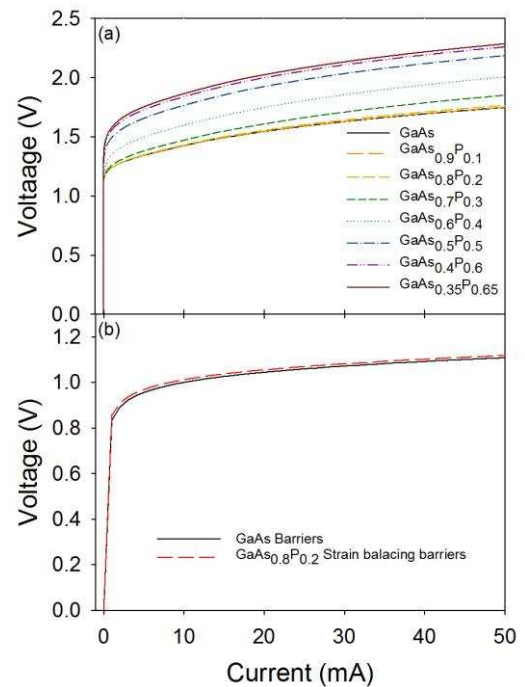


Fig. 5(a). Modelled IV characteristics for different phosphorus percentages in a 5nm strain balancing layer.

Fig. 5(b). Room temperature IV for QD mesa diodes fabricated from sample A and A'

A. Modelling

Finite element analysis simulations using RSOFT LaserMOD was used to model the effect of placing a GaAsP barrier between two quantum wells (QWs). QWs were used for simplicity and similar effects would be expected in QD structures with a wetting layer emission around $0.98 \mu\text{m}$. The cladding layer structure used is identical to the grown structures.

Figure 5 (a) shows modelled characteristics of a double $7.6 \text{nm In}_{0.19}\text{Ga}_{0.81}\text{As}$ QW emitting at $0.98 \mu\text{m}$ with a 5nm GaAsP barrier placed between the QWs. As the phosphorous content is increased from 0-20% there is no observable change in the IV behaviour. This is due to the height of the barrier produced by the $\text{GaAs}_{0.8}\text{P}_{0.2}$ being low enough not to impede carrier transport. Increasing the phosphorous content from 20-65% increases both the turn-

on voltage and internal resistance; both are detrimental effects. These modelling results indicate that a 5 nm thick GaAs_{0.8}P_{0.2} strain balancing layer should not adversely affect the electrical properties of a laser device. Figure 5 (b) shows experimental room temperature IV characteristics for mesa diodes containing 5 QD layers. Characteristics for samples A and A' are shown with no significant differences, in agreement with the conclusions from the modelling. This result demonstrates that GaAs_{0.8}P_{0.2} can be used to achieve strain balancing with no degradation of the electrical properties.

B. X-Ray Diffraction Analysis

X-Ray diffraction (XRD) measurements of all four samples were recorded using a Bruker D8 diffractometer. Symmetric scan measurements of ω -2 Θ were obtained along the [004] reflections to determine the out of plane strain. Spectra are shown in Figure 6.

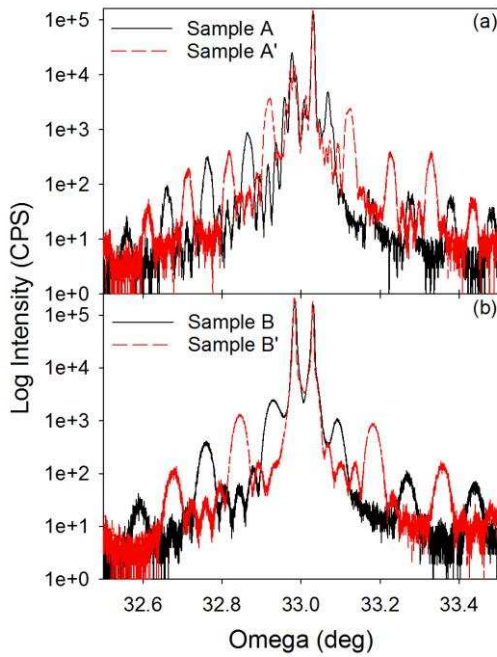


Fig. 6(a). XRD spectra of samples A & A'.
Fig. 6(b). XRD spectra of samples B & B'.

To understand how much strain balancing was needed, the total strain observed in sample A is calculated by analysis of the position of the strain peak with respect to the substrate peak. The two most dominant peaks are associated with the GaAs substrate at 33.03° and the AlGaAs cladding layer at 32.9732°. Fringe peaks arise from the repeating thickness of the active layer in the structure, which is the spacing thickness plus the thickness of the QD layer. Because this thickness does not change between samples the fringe spacing is constant. The thickness can be found using equation 1 where λ is the X-Ray source wavelength, θ_n is the n^{th} fringe peak and d is the thickness. The calculated thickness is 50nm, which is in agreement with measurements taken from TEM images and that intended from the growth. From table 1 the difference between the strain peak and the substrate peak can be found and the thickness of GaAs_{0.8}P_{0.2} can be calculated from equation 2.

$$n\lambda = 2d \sin \theta_n \quad (1)$$

$$t_{sb} = t_{sl} \frac{\Delta\theta_{split} \cot \theta_{GaAs}}{\Delta a/a} \quad (2)$$

where t_{sb} is the thickness of the GaAs_{0.8}P_{0.2}, $\Delta\theta_{split}$ is the difference between the substrate peak and the strain peak, θ_{GaAs} is the Bragg angle for GaAs, t_{sl} is the thickness of the strained layer, Δa is the change in lattice parameter and a is the lattice parameter of GaAs.

From analysis of sample A and from the calculation using equation 2, 5nm of GaAs_{0.8}P_{0.2} is used to compensate the strain caused by the QDs. Sample A' is identical to A but with the addition of 5nm GaAsP between the QD layers. Figure 6(a) shows that successful strain balancing has been achieved for sample A' with the Z₀ peak shifting to 33.02°, almost coinciding with the substrate peak at 33.03°.

A similar analysis can be used in Figure 6(b). Here a difference in repeat thickness is observed, with the fringe spacing being reduced to 30nm, agreeing again with TEM analysis. The increase in splitting between the Z₀ and substrate peak is due to the reduced spacing thickness causing a relatively larger indium concentration in the overall repeat structure. Therefore, the same thickness of GaAs_{0.8}P_{0.2} can be used to reduce the strain to almost zero.

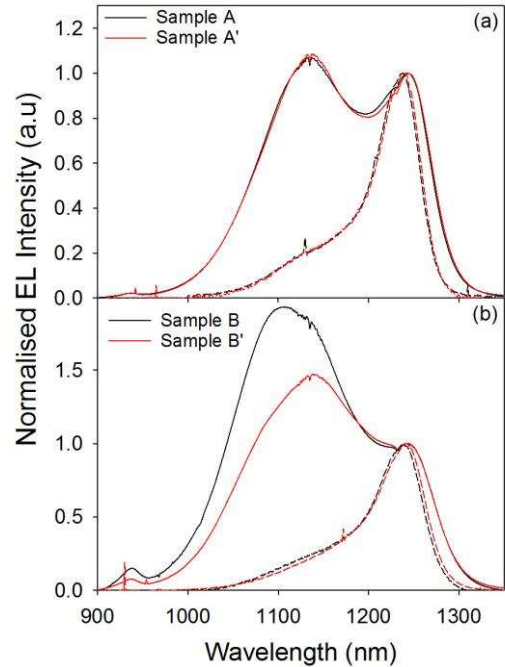


Fig. 7(a). Room temperature low and high current CW EL of samples A & A'.
Fig. 7(b). Room temperature low and high current CW EL of samples B & B'.
The spectra have been normalised to the ground state emission intensity.

C. Optical Characterisation of Mesa Diode Structures

400 μ m diameter mesa diodes were fabricated and tested at room temperature, using a continuous-wave (CW) current source at 1 and 100mA. Emitted light is detected by a liquid nitrogen cooled germanium detector. Figure 7(a) and (b) show normalised electroluminescence (EL) emission of all four samples at both low and high excitation current. Samples A and A' show similar emission spectra, indicating that there is no detrimental effect arising from incorporation of the GaAs_{0.8}P_{0.2} layer. Samples B and B' show similar low excitation spectra indicating that the GaAsP layer has not affected the ground state emission which will be responsible for the lasing transition. At high current the excited state emission from sample B' is relatively weaker in comparison to the ground state emission than is the case for sample B. The reason for this difference is unclear although it would

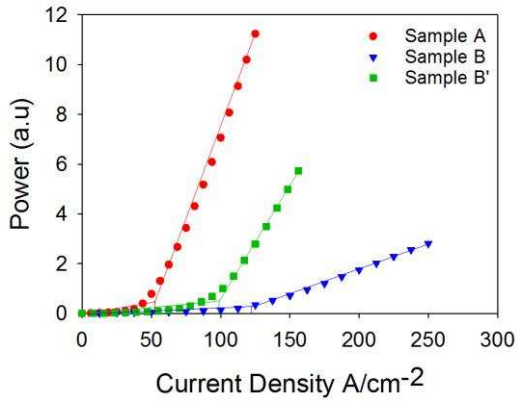


Fig. 8. Light power as a function of current for samples A, B & B' at 130K.

be consistent with a slightly higher QD density in sample B'. However, there is no structural data to support this.

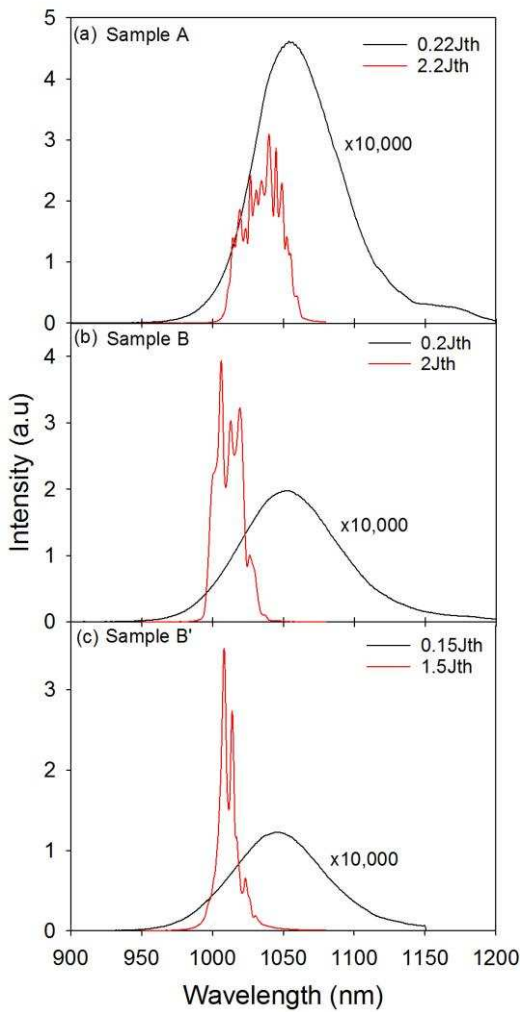


Fig 9. Above and below threshold emission spectra at 140K for the three laser devices studied.

IV. LASER RESULTS

Broad area lasers were fabricated from Samples A, B and B'. Sample A was fabricated into a 8mm x 50µm, Sample B was fabricated into a 8mm x 100µm ridge and sample B' was fabricated into a 8mm x 80µm ridge. Devices were tested in a cryostat over a range of temperatures, using a pulsed current source with a pulse width of 10µs and a duty

cycle of 1% to reduce heating effects. Figure 8 shows typical LvsJ characteristics measured at 130K. Values of 50A/cm², 125A/cm² and 100A/cm² are obtained for samples A, B & B' respectively. The lowest J_{th} value is obtained for sample A. Reducing the QD layer separation to 30 nm (B and B') increases J_{th} but this increase is significantly less for the sample with the GaAs_{0.8}P_{0.2} strain balancing layer (sample B'). This suggests that the GaAs_{0.8}P_{0.2} layer is beneficial for a spacing of 30nm but that further work is needed to achieve the quality obtained for 50nm spacing. Emission spectra recorded below and above threshold at 130K are shown in Figure 9 (a), (b) & (c). All spectra show lasing on the high energy shoulder of the below threshold emission, indicating that lasing is via an excited state and that there is insufficient ground state gain. Multiple lasing modes are observed due to the non-selective nature of the broad area laser.

Figure 10 shows the temperature variation of J_{th}. All three

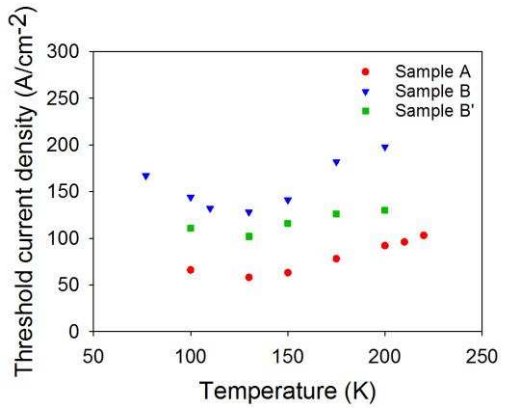


Fig. 10. Threshold current density as a function of temperature for samples A, B & B'.

samples exhibit a minimum J_{th} around 125K. The highest temperatures that lasing is achieved is 220K for sample A and 200K for samples B and B'; limited by the range of the current source. Over the studied temperature range J_{th} for sample B' is lower than for sample B providing further support for the benefits of the strain compensating GaAs_{0.8}P_{0.2} layer [28]. Coating the facets of the lasers with a high reflective coating is expected to result in room temperature operation of these devices. However further spectroscopic studies (presented in the next section) suggested that further QD optimisation is required to realise high performance room temperature strain balanced MOVPE grown QD lasers emitting at 1.3µm.

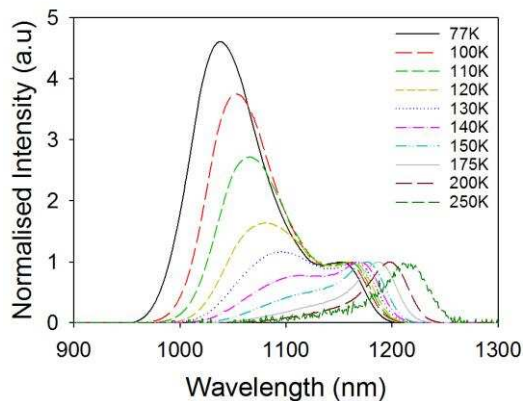


Fig. 11. Temperature dependence spectra of sample A using low excitation current.

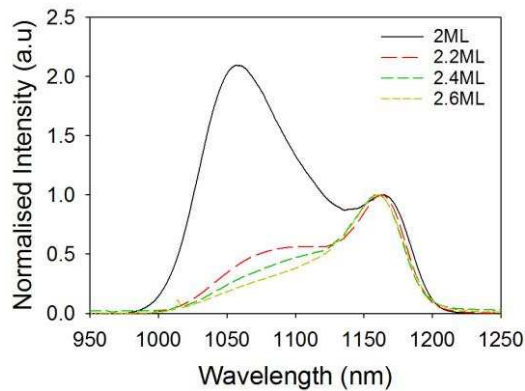


Fig. 12. Low temperature EL as a function of wavelength for different InAs coverages to give a reduction in QD bimodality. The spectra have been normalised to the long wavelength emission intensity.

V. QD BIMODALITY

Low temperature, low excitation current EL obtained from sample A is shown in Figure 11 for a range of temperatures. At these low currents and particularly at low temperatures all the QDs will be randomly populated by carriers rather than preferentially occupying the large QDs with deeper confining potentials. The low current ensures that the average dot carrier occupancy is $\ll 1$. The spectra revealed that the QDs have a bimodal size distribution [29], [30]. At low temperature the emission exhibits two peaks reflecting two subsets of QDs. The long wavelength emitting, larger quantum dots are required for lasing at 1.3 μm but these appear to have a significantly lower density than the smaller, shorter wavelength emitting QDs. As the temperature is raised the relative intensity associated with the short wavelength peak is reduced with the longer wavelength peak becoming dominant above 140K [31], [32]. Although at high temperatures carriers will transfer preferentially into the long wavelength emitting QDs these results indicate that they represent only a small fraction of the total QD density and hence that the available gain close to 1.3 μm will be limited. The bimodal distribution of QDs may occur due to the preferential nucleation on the upper side of step edges as Zhou et al. have observed and Liang et al. have modelled [32], [33].

To achieve room temperature ground state lasing the bimodality of the QDs needs to be reduced. This can be achieved by depositing additional InAs to help ripen the QDs. Low temperature measurements of samples grown with different InAs amounts are shown in Figure 12. Increasing the amount of InAs from 2 to 2.6ML results in a significant reduction of the bimodality with the emission now dominated by the longer wavelength emitting subset of larger QDs. However, this reduction is achieved with a commensurate reduction in optical efficiency. Compared to the 2 ML sample the integrated EL is reduced by 13 and 91% for the 2.2 and 2.4 ML samples respectively. However, increasing the amount of InAs to 2.2 ML significantly improves the bimodality, with only a slight fall in EL intensity. Further devices will require a detailed optimisation of the long wavelength emission, balancing a reduction in the bimodality with the decreasing overall optical efficiency. With additional optimisation of the

growth parameters we believe that sufficient gain at long wavelength can be achieved.

VI. SUMMARY

Optimisation of the growth parameters of InAs QDs has been presented, with a focus on developing devices able to produce 1.3 μm ground state lasing at room temperature. A novel aspect is the addition of a $\text{GaAs}_{0.8}\text{P}_{0.2}$ strain compensation layer to allow close spacing of the QD layers in a GaAs matrix and increased laser gain. Device modelling allows the maximum P content to be identified and this is confirmed by experimental IV measurements. XRD analysis confirms that strain balancing has been achieved for layer spacing of 50 and 30 nm. Laser devices are grown and fabricated with and without the strain balancing layer. Incorporation of this layer is shown to improve the performance of a 30 nm spacing device although this is still inferior to that of a 50 nm device without strain balancing. Both strain balanced and non-strain balanced lasers operate up to at least 200K for 30nm separation and 220K for 50nm separation, without any facet coating. A strong QD bimodality is shown to limit the ground state gain for QDs emitting close to 1.3 μm . The bimodality can be improved by increasing the InAs coverage, showing promise for future room temperature ground state lasing devices and novel device applications.

ACKNOWLEDGEMENTS

This work was funded by the EPSRC. TEM measurements were provided by Integrity Scientific Ltd. (www.integrityscientific.com). T. S Roberts would like to thank S. Kumar and K. Kennedy for help during fabrication and B. Harrison for discussions about growth.

REFERENCES

- [1] Y. Arakawa and H. Sakaki, "Multidimensional quantum well laser and temperature dependence of its threshold current," *Appl. Phys. Lett.*, vol. 40, no. 11, pp. 939-940, 1982.
- [2] J. Tatebayashi, N. Hatori, H. Kakuma, H. Ebe, H. Sudo, A. Kuramata, Y. Nakata, M. Sugawara and Y. Arakawa, "Low threshold current operation of self-assembled InAs/GaAs quantum dot lasers by metal organic chemical vapor deposition," *Electron. Lett.*, vol. 39, no. 15 pp. 1130, 2003.
- [3] I. N. Kaiander, R. L. Sellin, T. Kettler, N. N. Ledentsov, D. Bimberg, N. D. Zakharov and P. Werner, "1.24 μm InGaAs/GaAs quantum dot laser grown by metalorganic chemical vapor deposition using tertiarybutylarsine," *Appl. Phys. Lett.*, vol. 84, no. 16, pp. 2292, 2004.
- [4] A. Passaseo, G. Maruccio, M. De Vittorio, R. Rinaldi, R. Cingolani and M. Lomascolo, "Wavelength control from 1.25 to 1.4 μm in $\text{In}_x\text{Ga}_{1-x}\text{As}$ quantum dot structures grown by metal organic chemical vapor deposition," *Appl. Phys. Lett.*, vol. 78, no. 10, pp. 1382, 2001.
- [5] N. Nuntawong, Y. C. Xin, S. Birudavolu, P. S. Wong, S. Huang, C. P. Hains, D. L. Huffker, "Quantum dot lasers based on a stacked and strain-compensated active region grown by metal-organic chemical vapor deposition," vol. 86, no. 19, pp. 193115, 2005.
- [6] D. Bhattacharyya, E. A. Avrutin, A. C. Bryce, J. H. Marsh, D. Bimberg, F. Heinrichsdorff, V. M. Ustinov, S. V. Zaitsev, N. N. Ledentsov, P. S. Kop'ev, Z. I. Alferov, A. I. Onischenko, and E. P. O'Reilly, "Spectral and dynamic properties of InAs-GaAs self-organized quantum-dot lasers," *IEEE J. Sel. Top. Quantum Electron.*, vol. 5, no. 3, pp. 648-657, 1999.
- [7] J. Tatebayashi, M. Ishida, N. Hatori, H. Ebe, H. Sudo, A. Kuramata, M. Sugawara and Y. Arakawa, "Lasing at 1.28 μm of InAs-GaAs quantum dots with AlGaAs cladding layer grown by metal-organic chemical vapor deposition," *IEEE J. Sel. Topics in Quantum Electron.*, vol. 11, No. 5, pp. 1027-1034, 2005.
- [8] D. Guimard, M. Ishida, D. Bordel, L. Li, M. Nishioka, Y. Tanaka, M. Ekawa, H. Sudo, T. Yamamoto, H. Kondo, M. Sugawara and Y. Arakawa, "Ground state lasing at 1.30 μm from InAs/GaAs quantum

- dot lasers grown by metal-organic chemical vapor deposition," *Nanotechnology*, vol. 21, no. 10, pp. 105604-105610, 2010.
- [9] T. Yang, M. Nishioka and Y. Arakawa, "Optimising the GaAs capping layer growth of 1.3 μ m InAs/GaAs quantum dots by a combined two-temperature and annealing process at low temperatures," *J. Cryst. Growth*, vol. 310, no. 24, pp. 5469-5472, 2008.
- [10] S. Park, J. Tatebayashi and Y. Arakawa, "Structural and optical properties of high-density ($>10^{11}/\text{cm}^2$) InAs QDs with varying Al(Ga)As matrix layer thickness," *Phys. E Low-dimensional Syst. Nanostructures*, vol. 21, no. 2-4, pp. 279-284, 2004.
- [11] K. Nishi, H. Saito, S. Sugou and J.-S. Lee, "A narrow photoluminescence linewidth of 21meV at 1.35 μ m from strain reduced InAs quantum dots covered by In_{0.2}Ga_{0.8}As grown on GaAs substrates," *Appl. Phys. Lett.*, vol. 74, no. 8, pp. 1111-1113, 1999.
- [12] J. Tatebayashi, M. Nishioka and Y. Arakawa, "Over 1.5 μ m light emission from InAs quantum dots embedded in InGaAs strain-reducing layer grown by metalorganic chemical vapor deposition," *Appl. Phys. Lett.*, vol. 78, no. 22, pp. 3469, 2001.
- [13] T. D. Germann, A. Strittmatter, T. Kettler, K. Posilovic, U. W. Pohl and D. Bimberg, "MOCVD of InGaAs/GaAs quantum dots for lasers emitting close to 1.3 μ m," *J. Cryst. Growth*, vol. 298, pp. 591-594, 2007.
- [14] A. Passaseo, M. De Vittorio, M. T. Todaro, I. Tarantini, M. De Giorgi, R. Cingolani, A. Taurino, M. Catalano, A. Fiore, A. Markus, J. X. Chen, C. Paranthoen, U. Oesterle and M. Ilegems, "Comparison of radiative and structural properties of 1.3 μ m In_xGa_{1-x}As quantum-dot laser structures grown by metalorganic chemical vapor deposition and molecular-beam epitaxy; Effect on the lasing properties," *Appl. Phys. Lett.*, vol. 82, no. 21, pp. 3632, 2003.
- [15] A. A. El-Emawy, S. Birudavolu, P. S. Wong, Y.-B. Jiang, H. Xu, S. Huang and D. L. Huffaker, "Formation trends in quantum dot growth using metal organic chemical vapor deposition," *J. Appl. Phys.*, vol. 93, no. 6, pp. 3529, 2003.
- [16] A. Strittmatter, T. D. Germann, T. Kettler, K. Posilovic, U. W. Pohl and D. Bimberg, "Alternative precursor metal-organic chemical vapor deposition of InGaAs/GaAs quantum dot laser diodes with ultralow threshold at 1.25 μ m," *Appl. Phys. Lett.* Vol. 88, no. 26, pp. 262104, 2006.
- [17] T. Yang, S. Tsukamoto, J. Tatebayashi, M. Nishioka and Y. Arakawa, "Improvement of the uniformity of self-assembled InAs quantum dots grown on InGaAs/GaAs by low-pressure metalorganic chemical vapor deposition," *Appl. Phys. Lett.*, vol. 85, no. 14, pp. 2753-2755, 2004.
- [18] H. Shin, J.-B. Kim, Y.-H. Yoo, W. Lee, E. Yoon and Y.-M. Yu, "Enhanced strain of InAs quantum dots by an InGaAs ternary layer in a GaAs matrix," *J. Appl. Phys.*, vol. 99, no. 2, p. 23521, 2006.
- [19] T. Kageyama, K. Watanabe, Q. H. Vo, K. Takesmasa, M. Sugawara, S. Iwamoto and Y. Arakawa, "InAs/GaAs quantum dot lasers with GaP strain-compensation layers grown by molecular beam epitaxy," *Phys. Status Solidi A*, vol. 213, no. 4, pp. 958-964, 2006.
- [20] J. Tatebayashi, N. Nutntawong, P. S. Wong, Y.-C. Xin, L. F. Lester, D. L. Huffaker, "Strain compensation technique in self-assembled InAs/GaAs quantum dots for applications to photonic devices," *J. Phys. D: Appl. Phys.* Vol. 42 no. 7, pp. 073002-073014, 2009.
- [21] N. Nuntawong, J. Tatebayashi, P. S. Wong and D. L. Huffaker, "Localised strain reduction in strain-compensated InAs/GaAs stacked quantum dot structures," *Appl. Phys. Lett.*, vol. 90, no. 16, pp. 163121, 2007.
- [22] N. Nuntawong, S. Huang, Y., B. Jiang, C. P. Hains and D. L. Huffaker, "Defect dissolution in strain-compensated stacked InAs/GaAs quantum dots grown by metalorganic chemical vapor deposition," *Appl. Phys. Lett.*, vol. 87, no. 11, pp. 113105, 2005.
- [23] P. Lever, H. H. Tan and C. Jagadish, "InGaAs quantum dots grown with GaP strain compensation layers," *J. Appl. Phys.*, vol. 95, no. 10, p. 5710, 2004.
- [24] N. H. Kim, P. Ramamurthy, L. J. Mawst, T. F. Kuech, P. Modak, T. J. Goodnough, D. V. Forbes, and M. Kanskar, "Characteristics of InGaAs quantum dots grown on tensile-strained GaAs_{1-x}P_x," *J. Appl. Phys.*, vol. 97, no. 9, p. 93518, 2005.
- [25] N.-H. Kim, J.-H. Park, L. J. Mawst, T. F. Kuech, and M. Kanskar, "Temperature sensitivity of InGaAs quantum-dot lasers grown by MOCVD," *IEEE Photonics Technol. Lett.*, vol. 18, no. 8, pp. 989-991, 2006.
- [26] R. Beanland, "Dark field transmission electron microscope images of III-V quantum dot structures," *Ultramicroscopy*, vol. 102, no. 2, pp. 115-125, 2005.
- [27] P. B. Joyce, T. J. Krzyzewski, G. R. Bell, T. S. Jones, S. Malik, D. Childs, and R. Murray, "Effect of growth rate on the size, composition, and optical properties of InAs/GaAs quantum dots grown by molecular-beam epitaxy," *Phys. Rev. B*, vol. 62, no. 16, pp. 10891-10895, 2000.
- [28] G. Park, D. L. Huffaker, Z. Zou, O. B. Shchekin and D. G. Deppe, "Temperature dependence of lasing characteristics for long-wavelength (1.3 μ m) GaAs-based quantum-dot lasers," *IEEE, Photonics Technol. Lett.*, vol. 11, no. 3, pp. 301-303, 1999.
- [29] I. O'Driscoll, P. Blood, and P. M. Snowton, "Random Population of Quantum Dots in InAs-GaAs Laser Structures," *IEEE J. Quantum Electron.*, vol. 46, no. 4, pp. 525-532, 2010.
- [30] M. Grundmann and D. Bimberg, "Theory of random population for quantum dots," *Phys. Rev. B*, vol. 55, no. 15, pp. 9740-9745, 1997.
- [31] H. Wang, D. Ning, and S. Feng, "Temperature dependence of the optical properties of InAs/GaAs self-organized quantum dots with bimodal size distribution," *J. Cryst. Growth*, vol. 209, no. 4, pp. 630-636, 2000.
- [32] F. Franchello, L. D. de Souza, E. Laureto, A. A. Quivy, I. F. L. Dias, and J. L. Duarte, "Influence of bimodal distribution and excited state emission on photoluminescence spectra of InAs self-assembled quantum dots," *J. Lumin.*, vol. 137, pp. 22-27, 2013.
- [33] S. Liang, H. L. Zhu, and W. Wang, "Size distributions of quantum islands on stepped substrates," *J. Chem. Phys.*, vol. 131, no. 15, p. 154704, 2009.
- Timothy S. Roberts** received the M.Eng. degree in microelectronics from the University of Sheffield, Sheffield, U.K., in 2013, where he is currently working toward the Ph.D. degree in MOVPE growth of Quantum Dots.
- Benjamin J. Stevens** received the Ph.D. degree in advanced GaAs-based lasers from the University of Sheffield, Sheffield, U.K., in 2010. Since July 2009, he has been at the National Centre for III-V Technologies, University of Sheffield, where he is responsible for the development of MOVPE growth. His research interests include lasers and regrowth technologies. He received the Japanese Society for the Promotion of Science Summer Fellowship, which he spent in the Asakawa Group, Tsukuba, Japan, learning selective area MBE.
- Edmund Clarke** received the B.Sc. degree in physics and the Ph.D. degree in physics from Imperial College London, London, U.K., in 1996 and 2005, respectively. He was a Research Associate at Imperial College London for five years, where he was involved in the research on molecular beam epitaxy of quantum dot devices. In October 2010, he joined EPSRC National Centre for III-V Technologies, University of Sheffield, Sheffield, U.K., where he is currently a Research Fellow, and is responsible for III-V semiconductor growth by molecular beam epitaxy.
- Ian Tooley** graduated with his first degree, a BSc in Electronics at University of Salford in 1978. He graduated in 1986 with an MSc in microelectronics from University of Surrey in 1986. Since then he has worked in roles as technical support, technical sales, owning & running his own international telecoms company, running and owning his own management consultancy, sitting on advisory boards to the international telecoms industry and European photonics helping steer funding for Horizon 2020. He is currently researching for a PhD in semiconductor lasers.
- Jonathan Orchard** received the M.Eng. degree in electronic engineering and the Ph.D. degree from the University of Sheffield, Sheffield, U.K., where he was involved in the design and characterization of vertical cavity lasers in 2008 and 2012, respectively. He was a Postdoctoral Researcher at the University of Sheffield where he was involved in research on various aspects of quantum dot photonic devices grown on silicon substrates, including

carrier dynamics and long wavelength emission. He is currently with the University of Glasgow.

Ian Farrer received the M.Sci. degree in physics and Ph.D degree from the University of Cambridge. He is Lecturer of Semiconductor Epitaxy and Materials in the Electronic and Electrical Engineering Department at the University of Sheffield. He has been a key member of the collaboration between the University of Cambridge and Toshiba Research Europe for over 15 years, leading the growth programme for the last 9 years. He is expert on both the growth of self-assembled quantum dots and of ultra-high mobility materials for fundamental transport experiments at low temperatures. His work has led to the creation of charge tuneable structures leading directly to the demonstration of two photon interference from remote quantum dot devices. Similarly his p-i-n structures were used in the fabrication of the first entangled-photon light emitting diode, and recently to demonstrate quantum teleportation.

David T.D Childs received the B.Sc. degree in physics, the M.Sc. degree in semiconductor science and technology, and the Ph.D. degree from Imperial College, London, U.K., in 1996, 1997, and 2002, respectively. He was with the R&D Department of Marconi Optical Components and Bookham, Caswell Semiconductor Research and Fabrication Facility, till 2006, where he was responsible for the development of a range of telecommunication lasers. He was with the Department of Electronic and Electrical Engineering, University of Sheffield, Sheffield, U.K. until September 2015. Since then he has been at the University of Glasgow. He is involved in a number of projects developing semiconductor light sources from visible to terahertz wavelengths. This work spans from fundamental material improvement to advanced device engineering. He is also involved in the application of semiconductor devices to fields ranging from selective laser melting to mid-infrared hyperspectral imaging.

Nasser Babazadeh received the Ph.D. degree from the University of Sheffield, Sheffield, U.K., in 2010. Since 2010, he has been a Postdoctoral Researcher with the Department of Electronic and Electrical Engineering, University of Sheffield until December 2015. Since then he has been working at the University of Glasgow. His research interests include semiconductor nanostructures, with emphasis on quantum dot, quantum well structures including VCSELS/VECSELS, and super luminescent diodes.

Nobuhiko Ozaki received a B.Sc. degree in physics in 1997, and M.Sc. and Ph. D. degrees in physics in 1999 and 2002, respectively, all from Osaka University, Japan. In 2002, he joined the Institute of Materials Science, University of Tsukuba, Japan as a Research Associate. In 2005, he joined the Center for Tsukuba Advanced Research Alliance (TARA), University of Tsukuba, Japan as an Assistant Professor. In 2009, he moved to the Faculty of Systems Engineering, Wakayama University, Japan as an Associate Professor. From 2014 to 2015, he was a Visiting Academic in the Department of Electronic and Electrical Engineering, the University of Sheffield, Sheffield, UK. His current research includes the selective-area-growth of quantum dots and their application to near-infrared

broadband light sources for optical coherence tomography applications.

David Mowbray received B.A. and D.Phil. degrees from Oxford University, Oxford, U.K., in 1984 and 1989, respectively. His D.Phil. research was focused on the optical properties of InGaAs-InP quantum-well systems. From 1989 to 1990, he held an Alexander von Humboldt Fellowship at the Max Planck Institute for Solid State Research, Stuttgart, Germany. Since 1991, he has been a member of the Department of Physics and Astronomy, University of Sheffield, Sheffield, U.K. His current research interests include the development of long wavelength InAs quantum-dot emitters and the development of nanowire QDs.

Richard A. Hogg received the Ph.D. degree in physics from the University of Sheffield, Sheffield, U.K., in 1995. He was a Postdoctoral Researcher with NTT Basic Research Laboratories, Atsugi, Japan, for two years. He was with Toshiba Research Europe's Cambridge Laboratory for three years. In 2000, he joined Agilent Technologies Fibre-Optic Component Operation, Ipswich, U.K. In 2003, he joined the Electronic and Electrical Engineering Department, University of Sheffield, where he stayed until August 2015. He is currently a Professor of semiconductor devices at the University of Glasgow. His research group is active in developing the understanding of device physics and engineering, epitaxial processes fabrication technologies, and applications of various semiconductor laser, amplifier, and superluminescent diode devices. He received an EU-Japan Fellowship as a Visiting Researcher in Professor Arakawa's Laboratory, University of Tokyo.

